

Diverse Deep Feature Ensemble Learning for Omni-Domain Generalized Person Re-identification

Eugene P.W. Ang*

Rapid-Rich Object Search (ROSE) Lab,
Nanyang Technological University
Singapore, Singapore
phuaywee001@e.ntu.edu.sg

Shan Lin

Rapid-Rich Object Search (ROSE) Lab,
Nanyang Technological University
Singapore, Singapore
shan.lin@ntu.edu.sg

Alex C. Kot

Rapid-Rich Object Search (ROSE) Lab,
Nanyang Technological University
Singapore, Singapore

ABSTRACT

Person Re-identification (Person ReID) has progressed to a level where single-domain supervised Person ReID performance has saturated. However, such methods experience a significant drop in performance when trained and tested across different datasets, motivating the development of domain generalization techniques. However, our research reveals that domain generalization methods significantly underperform single-domain supervised methods on single dataset benchmarks. An ideal Person ReID method should be effective regardless of the number of domains involved, and when test domain data is available for training it should perform as well as state-of-the-art (SOTA) fully supervised methods. This is a paradigm that we call *Omni-Domain Generalization* Person ReID (ODG-ReID). We propose a way to achieve ODG-ReID by creating deep feature diversity with self-ensembles. Our method, Diverse Deep Feature Ensemble Learning (D²FEL), deploys unique instance normalization patterns that generate multiple diverse views and recombines these views into a compact encoding. To the best of our knowledge, our work is one of few to consider omni-domain generalization in Person ReID, and we advance the study of applying feature ensembles in Person ReID. D²FEL significantly improves and matches the SOTA performance for major domain generalization and single-domain supervised benchmarks.

CCS CONCEPTS

- Information systems → Image search; • Computing methodologies → Visual content-based indexing and retrieval.

KEYWORDS

person re-identification, domain generalization, ensemble learning

ACM Reference Format:

Eugene P.W. Ang, Shan Lin, and Alex C. Kot. 2024. Diverse Deep Feature Ensemble Learning for Omni-Domain Generalized Person Re-identification. In *2024 9th International Conference on Multimedia and Image Processing (ICMIP) (ICMIP 2024), April 20–22, 2024, Osaka, Japan*. ACM, New York, NY, USA, 8 pages. <https://doi.org/10.1145/3665026.3665036>

*Corresponding author.

Permission to make digital or hard copies of part or all of this work for personal or classroom use is granted without fee provided that copies are not made or distributed for profit or commercial advantage and that copies bear this notice and the full citation on the first page. Copyrights for third-party components of this work must be honored. For all other uses, contact the owner/author(s).

ICMIP 2024, April 20–22, 2024, Osaka, Japan

© 2024 Copyright held by the owner/author(s).

ACM ISBN 979-8-4007-1616-4/24/04.

<https://doi.org/10.1145/3665026.3665036>

1 INTRODUCTION

Person Re-identification (ReID) is the task of matching images of a person captured across multiple non-overlapping cameras. In single-domain ReID, methods are trained and tested on the same multi-camera system (domain) with mutually exclusive person identities between training and testing sets. A key disadvantage of conventional single-domain ReID methods is that they generally perform worse when tested on other domains (e.g., the mAP drops from 76.3 to 16.1 as shown in Table 1), motivating the development of cross-domain ReID methods that assume the training and testing sets come from different domains. This is a step toward practical application as it approximates real-world constraints such as having limited or no access to data in the target domain. However, cross-domain methods can have overly specialized requirements such as having access to multiple source domains for training. Table 1 reveals that state-of-the-art (SOTA) cross-domain methods do well when tested on unseen domains but under-perform simple baselines when testing on the original source domains. For example, when a recent SOTA method ACL [33] is trained on a mix of datasets that include DukeMTMC-reID, it can only achieve a mAP of 72.9 when tested on the DukeMTMC-reID test set, which is lower than the simple Bag-of-Tricks (BoT) baseline performance [21]. Our goal for this work is to investigate Person ReID methods that can achieve strong performance regardless of domain setting. The ideal ReID methods should perform well in both single domain setting and cross-domain setting, while still performing well in the original training domain. We refer to such methods as Omni-Domain Generalized ReID (ODG-ReID) methods.

Table 1: The performance of single-domain methods degrades when testing on other datasets, while cross-domain generalization methods cannot maintain the same performance on the original training dataset. All results are in mAP and the best result for each benchmark is bold. Dataset abbreviations: M is Market-1501 [35], D is DukeMTMC-reID [37], C is CUHK03 [16] and MS is MSMT17_V2 [28].

Setting	Methods	Single Domain Train		Multi-Domain Train	
		D → D	M → D	C+D+M → D	C+M+MS → D
Normal	Baseline (BoT) [21]	76.3	16.1	76.3	38.6
DG	DualNorm [12]	67.7	23.9	76.3	40.5
	META [30]	46.7	18.3	60.6	42.7
	ACL [33]	49.9	22.2	72.9	53.4
	SIL [26]	61.5	25.1	65.6	47.0

Our method re-investigates the use of Instance Normalization (IN), a technique popularly used in Domain Generalization Person ReID (DG-ReID) methods [12]. IN normalizes the style attributes

of images so that models learn domain-invariant features and ignore domain-specific style cues that lead to overfitting. First proposed for DG-ReID in DualNorm [12], IN layers were added to the early blocks of the network but not to the later layers because the former seemed to perform better. While this design decision is superior in some benchmarks, we uncover a more complicated story: unconventional applications of IN can also achieve superior performance in other benchmarks. Table 2 illustrates how IN is applied in the bottlenecks of a ResNet [8] and enumerates all possible IN-combinations on the final two bottlenecks. Trying these four combinations on two example benchmarks, the table in Figure 1 shows that adding IN in the later bottlenecks can be beneficial. In this table, different IN patterns excel in different benchmarks regardless of domain setting. Ultimately, no single IN pattern is superior in all cases. Based on these findings, a successful method has to consider different IN patterns *all at the same time* in order to do well for unseen target benchmarks. Our method, the Diverse Deep Feature Ensemble Learning (D²FEL), uses self-ensembling to achieve this simultaneous diversity: each subhead applies a unique IN pattern and they collectively view the input through the lens of all possible IN-combinations.

Table 2: Various IN-patterns are applied to the final bottleneck layers of a backbone ResNet-50 and each pattern is evaluated on same-domain and cross-domain benchmarks. No single pattern (column) outperforms the rest consistently in all benchmarks (row). Results are in Rank-1 and the best of each benchmark is bold. Columns correspond to the branch labels in Figure 1.

	No-IN	IN-Last	IN-2nd-Last	IN-Last-Two
M → M	92.5	94.3	93.1	94.2
C → C	90.6	89.0	88.1	90.4
MS → MS	79.0	79.3	79.4	80.5
D → MS	41.1	35.4	38.9	36.0
M → MS	30.6	30.3	31.4	31.0
C → MS	33.4	35.3	33.0	37.6

Self-ensembles are a resource-efficient way to perform ensemble learning. As Figure 2 illustrates, the subheads in self-ensembles are copies of the original network head sharing the early layers of a feature extraction backbone. Such a structure reduces memory use and enables training of the ensemble all in one go. Initially proposed for image classification tasks [15] and used to perform knowledge distillation in ReID [17], we found no works that studied how to directly apply self-ensembles for inference in ReID. The usual way to apply ensemble techniques in image classification is to average the predicted class logits from different subheads as the ensemble’s own prediction. A naive extension to ReID would be to average the output *features* of all subheads instead, using the averaged feature as a search key. Experimentally, this yields poor results and the reason for this is that it makes sense to average class logits, but not features. In the former case, each logit component corresponds to the confidence score for a particular person’s identity. Taking the average of these logits makes sense because there is a perfect correspondence between logits produced by different

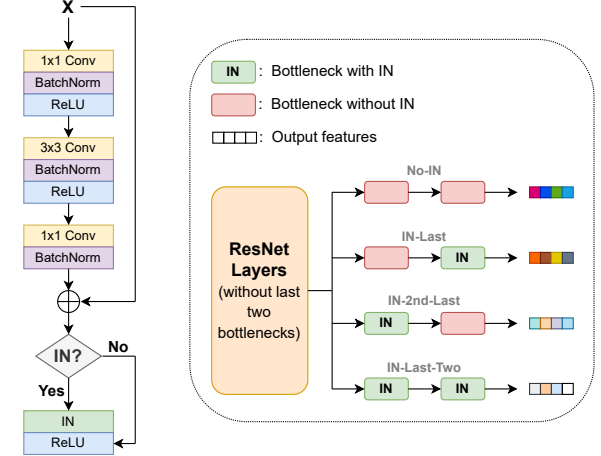


Figure 1: Left: Structure of a bottleneck layer in a ResNet [8], where IN can be selectively applied at the end. Right: all possible IN-combinations applied to the final two bottlenecks of the network.

models. In the latter case, however, features from different subheads are not necessarily aligned along their coordinate axes and averaging them degrades performance, as Figure 3 (left) illustrates and the experiment on the right confirms. We found that it was better to concatenate all features together to preserve their information. To the best of our knowledge, our work is the first to propose the application of self-ensembles in Person ReID inference.

As the number of subheads increase, concatenating their features together can be impractical due to the large features produced. We propose an effective way to reduce their dimensions using the Johnson-Lindenstrauss (JL) lemma [14]. The JL-lemma relates the dimension reduction of a set of data points to the conservation of pairwise distances between the same points in the reduced space. By performing a random projection from a high dimension D down to a lower dimension d , we only sacrifice a small amount of performance even when the reduction is very wide, e.g. $D = 16384$, $d = 2048$. No training cost is incurred, making this a cost-effective method. One disadvantage of random projections, however, is that as d gets very small the quality of the reduced features drops sharply.

If minimal performance loss is desired, we found that traditional dimension reduction models designed to minimize information loss such as Principal Component Analysis (PCA) work very well. Such principled techniques work well regardless of the training set provided (assuming a sufficient sample size), generalizing well to unseen domains with minimal loss in performance. Furthermore, PCA-reduced features maintain strong performance even down to very small dimensions, making it ideal for applications that need lean search features. Training a PCA model only incurs a one-time effort after D²FEL is trained and is relatively fast.

Finally, our experiments reveal that deep learning dimension reduction techniques such as auto-encoders perform well in same-domain settings but perform poorly in cross-domain settings. This suggests that deep-learning approaches to dimension reduction have a tendency to overfit to the training set by exploiting domain

specific information during the encoding process, but ignore important domain generalizable details. We propose traditional reduction techniques since they are mathematically formulated to preserve information during reduction. Table 7 performs a comparison of dimension reduction techniques across various benchmarks.

To summarize, our contributions are as follows:

- We propose D²FEL, a framework that extracts rich and diverse views of data with a self-ensemble architecture. To the best of our knowledge, we are the first to apply feature ensembles directly for Person ReID inference and search.
- We pioneer the novel adoption of the principled *Random Projection* reduction technique into Person ReID, enabling practical use of feature ensembles in ReID.
- Our method D²FEL outperforms the state-of-the-art (SOTA) in several multi-source domain generalization Person ReID benchmarks while still matching or surpassing the SOTA performance for single domain Person ReID benchmarks, demonstrating Omni-Domain Generalization.

2 RELATED WORK

Single-Domain Person Re-identification Single-domain Person ReID benchmarks, which train and test models within a single multi-camera system (domain), are among the earliest efforts of the Person ReID community. Such modern methods are mostly based on deep convolutional neural networks. Early deep learning based work usually formulated Person ReID as a verification problem and proposed Siamese architectures [11, 16, 19]. In recent years, verification-driven triplet architectures such as [2, 9] overtook Siamese structures due to their robustness. Another popular approach uses the classification loss: Zheng et al. [36] first proposed the ID-Discriminative Embedding (IDE) to finetune ImageNet [6] pretrained models to classify person IDs. More recent approaches [21, 27, 31] combine both classification loss and verification loss.

Domain-Generalized Person ReID: A task that has been gaining traction in the field of Person ReID, Domain-Generalized Person ReID (DG-ReID) aims to learn a model that can generalize well to unseen target domains without involving any target domain data for adaptation. IBN-Net [23] first introduced the instance normalization (IN) layer to normalize the style and content variations within the image batch during the training. This was later applied to DG-ReID by DualNorm [12]. MMFA-AAE [20] used a domain adversarial learning approach to remove domain-specific features. Later DG methods such as DIMN [25], QACConv [18], M³L [34] used hyper-networks or meta-learning frameworks coupled with memory bank strategies. DEX [1] proposed a deep feature augmentation loss that implicitly transforms intermediate deep features over expected Gaussian noise perturbation. ACL [33] propose a module that captures then fuses domain invariant and domain specific features, which is plugged into different layers of a generic feature extractor as a replacement for selected conv blocks. Style Interleaved Learning (SIL) [26] is a recent method that employs an additional forward pass during training to interleave feature styles. Finally, methods like RaMoE [4] and META [30] deploy a mixture of experts to specialize to each domain, with META being a more lightweight variant because of extensive parameter sharing.

Our method D²FEL is most similar in concept to mixture of experts because we deploy a diverse mix of specialized network subheads.

Self-Ensembles Self-ensembles were first proposed by ONE [15] for image classification, which extended a base network with auxiliary branches that each generate logits to be used as soft labels for knowledge distillation. RESL [17] applied a similar architecture for domain adaptation in Person ReID, also using it for knowledge distillation. In both methods, the auxiliary branches are discarded after knowledge distillation in order to reduce computation. Our method differs from them because we use self-ensembles not for knowledge distillation, but as a way to extract rich and diverse features from the input. Our work is the first to explore how self-ensemble features can be directly used for inference and search in Person ReID instead of discarding the auxiliary branches.

Dimension Reduction The JL-Lemma tells us that when a set of high-dimensional points are randomly projected to a lower dimension, their pairwise distances are preserved up to a bounded error that depends mainly on the size of the target dimension [5, 14]. The solid theoretical foundations of the JL-Lemma gives strong guarantees of the feasibility of random projections as a real-time dimension reduction tool. In this study, we demonstrate the potential of random projections as a practical component in a Person ReID framework. Principal component analysis (PCA) [7, 10] linearly projects datasets into smaller subspaces while retaining the directions of greatest variance.

3 METHODOLOGY

We are given a dataset of person images with identity labels $D = \{x_i, y_i\}_1^n$. A model f maps images to feature encodings - for this work, we fix f to be a ResNet-50, which is made up of bottleneck components as illustrated in Figure 1. We refer to these bottlenecks using indices counting backwards from the output of the network. For example, bottleneck-1 is the last layer and bottleneck-2 comes before bottleneck-1.

3.1 Instance Normalization (IN) Patterns

A key feature of D²FEL is the ability to apply varying patterns of IN to the subhead bottlenecks. Given an input batch $x \in \mathbb{R}^{B \times C \times H \times W}$ with b indexing batch size B , c indexing number of channels C , spatial dimensions H, W , and a small value ϵ for numerical stability, an IN operation is specified as:

$$\text{IN}(x_{bc}) = \frac{x_{bc} - \mu_{bc}}{\sqrt{\sigma_{bc}^2 + \epsilon}}, \quad (1)$$

$$\mu_{bc} = \frac{1}{HW} \sum_{i=1}^W \sum_{j=1}^H x_{bcij}, \quad (2)$$

$$\sigma_{bc}^2 = \frac{1}{HW} \sum_{i=1}^W \sum_{j=1}^H (x_{bcij} - \mu_{bc})^2 \quad (3)$$

In each bottleneck layer, we have a choice to apply IN or not. Our experiments indicate that using a diverse set of IN combinations generates a richer set of features that consistently perform well across extensive Person ReID benchmarks. We introduce the concept of Fully-Combinatorial-IN for a depth $\delta \in \mathbb{Z}^+$ as the simultaneous application of all 2^δ IN-combinations on bottlenecks- $(\delta, \delta-1, \dots, 1)$.

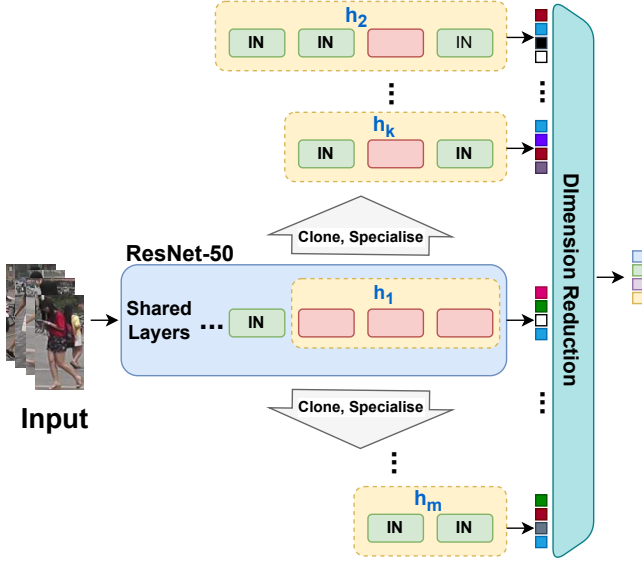


Figure 2: A summary of our D²FEL framework, which uses partial copies of itself to form an ensemble. Each copy is specialized with a unique pattern of instance normalization.

Figure 1 illustrates Fully-Combinatorial-IN for $\delta = 2$. The table in Fig 1 compares the effect of changing IN-patterns in the last two bottlenecks over several benchmarks, showing that it is impossible to predetermine patterns that work for all target domains. Thus, a Fully-Combinatorial-IN strategy spanning all patterns is the best solution to this uncertainty. One of the ways we can implement Fully-Combinatorial-IN is to train multiple models, each using a different IN pattern. Our method D²FEL takes a leaner approach and achieves this with self-ensembles.

3.2 Our Method: D²FEL

Figure 2 illustrates our method, D²FEL. We fix the main backbone f and clone $m - 1$ subheads $\{h_k\}_2^m$ from the final bottlenecks of f for a total of m heads. All subheads share the earlier layers of f . For each subhead, we can specify the start point $\{f_k\}_2^m$ to duplicate from and the IN-pattern. This design gives the flexibility to express just a subset of all possible IN patterns for more lightweight requirements. We define $f := h_1 \circ f_1$. Given an input image x , the D²FEL function ω produces a collection of features, one from each of the m heads:

$$\omega(x) = \{h_k(f_k(x))\}_1^m \quad (4)$$

For classification tasks, these subheads are usually linearly projected into class logits and averaged for knowledge distillation or testing. In Person ReID, we want to directly use the features for retrieval instead. Figure 3 demonstrates, however, that taking average of features in this naive manner is detrimental: the performance of the averaged feature is no better than individual subhead features. Instead, if we were to use the *logits* as retrieval vectors, the performance of the average of all logits is far better than that of an individual logit. This is because logit components are aligned with each other, as each component refers to the same person identity across all subheads, while feature components do not necessarily follow such alignment. Therefore, instead of taking a mean of the

features we concatenate them together into larger features:

$$\Omega(x) = \|\Omega(x)\|_1^m \quad (5)$$

While $\Omega(x)$ can be directly used for the Person ReID search, as the number of subheads increases it can grow very large, motivating the need for good dimension reduction techniques to efficiently reduce $\Omega(x)$ to a practical size.

3.3 Dimension Reduction

A set of m omni-normalized features from D²FEL each with 2048-dimensional features would have a combined dimension of $D = 2048m$ that needs to be reduced to be practical. We found that deep learning solutions for dimension reduction, such as deep auto-encoders, performed well in single-domain Person ReID but not as well across domains, indicating an overfit to the training domain. Instead, we found that older methods in the literature, such as principal component analysis and random projections, were more robust to ever-changing domain settings. Furthermore, to the best of our knowledge, we are the first to adapt random projection techniques, traditionally applied in the field of database search, for Person ReID. We present our study of these techniques in the following sections.

3.3.1 Deep Auto-Encoders. Figure 4 illustrates the basic design of the deep auto-encoder experiments we conducted for dimension reduction. We train the auto-encoder on the feature ensemble generated by D²FEL, using either L_1 or L_2 reconstruction loss. We use the compressed feature (coloured squares in the middle) for evaluation. Table 7 shows that deep learning dimension reduction methods overfit to the training set, performing well in single-domain Person ReID but performing poorly across domains.

3.3.2 Principal Component Analysis (PCA). PCA constructs an orthogonal basis from the eigenvectors of $\{\Omega(x)\}_1^n$ that maximally captures the information encoded in the features [7, 10]. By selecting the eigenvectors corresponding to the d largest eigenvalues, PCA maximally captures the diversity of the data in X using only d dimensions. While the training time of PCA grows with D , it is still only a fraction of the time taken to train deep learning models. Furthermore, this is a one-time cost - once trained, it can be deployed at the end of D²FEL, as illustrated in Figure 2. Compared with random projections, Figure 5 shows that PCA can preserve performance down to much smaller dimensions. Thus, PCA is an ideal solution if maximal performance or small but effective search features are desired.

3.3.3 Random Projections. Given a set of high dimensional features $\{\Omega(x)\}_1^N \in \mathbb{R}^D$, the Johnson-Lindenstrauss (JL) lemma states the conditions necessary for a random projection from dimension D to $d \ll D$ to preserve the pairwise distances between points in \mathbb{R}^D and their projected counterparts in \mathbb{R}^d . If these distances are preserved, any evaluation performed on the projected points in \mathbb{R}^d would be very close to evaluating the original high-dimensional points. A random projection matrix $U \in \mathbb{R}^{D \times d}$ can be constructed independently from data: $U_{ij} \sim \mathcal{N}(0, 1), \forall i, j$. We can define the projection $\Pi \in \mathbb{R}^D \times \mathbb{R}^d$ as: $\Pi(\Omega(x)) = U^\top \Omega(x)$. If $d \geq 24 \ln N(3\epsilon^2 - 2\epsilon^3)^{-1}$, then we can in randomized polynomial time find a projection Π such that the pairwise distances are preserved to within a tolerance

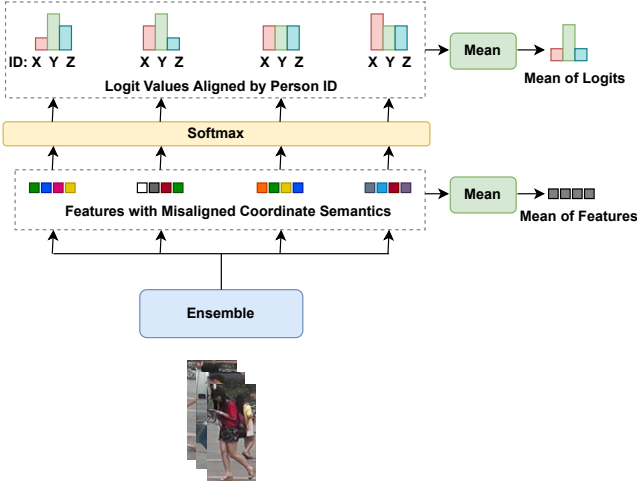


Figure 3: We compare the effects of averaging the coordinate values of class logits vs. regular output features. Even though logits do not perform as well as features for ReID, a pattern is clear: averaging class logits boost performance because they are semantically aligned by design, but averaging features reduces performance because their coordinates do not necessarily align.

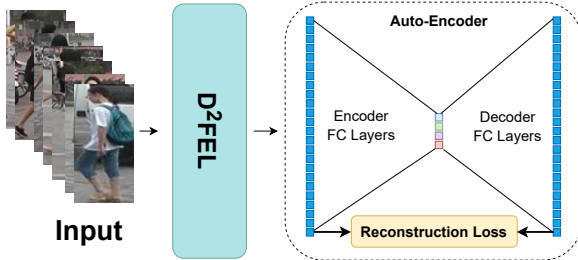


Figure 4: Design of our deep auto-encoder experiments.

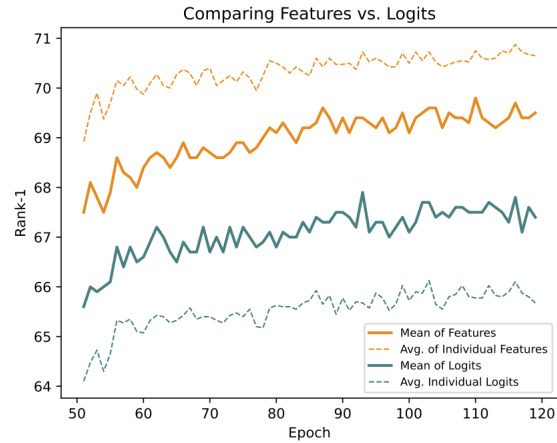
$$0 \leq \epsilon \leq 1 \text{ for all } u, v \in \{\Omega(x)\}_1^N [5]:$$

$$(1 - \epsilon)\|u - v\|^2 \leq \|\Pi(u) - \Pi(v)\|^2 \leq (1 + \epsilon)\|u - v\|^2 \quad (6)$$

For example, if the gallery we are searching has $N = 10000$ points and we wish to reduce feature dimensions down to $d = 2048$, then the JL-lemma guarantees the existence of a projection that achieves the error bound $\epsilon = 0.2$. For random projections, ϵ is independent of the original dimension D , which is a very useful property since the time taken to fit other dimension reduction models like PCA grows cubically with D , but random projections do not require training and achieve error rates of ϵ as long as we fix the target dimension d . While speed, convenience and performance are major plus points of random projections, there are trade-offs to consider. Firstly, there will still be a slight drop in performance. Secondly, the target dimension needs to be reasonably large otherwise performance drops severely (Figure 5), making random projections ill-suited for applications that require very small search features.

3.4 Loss Function

For each ensemble output feature $\omega_k(x)$ with label y , we apply three losses. First, we apply a cross-entropy loss over the person identity labels: $L_{CE} = -\log \frac{\exp w_y \cdot \omega_k(x)}{\sum_{j=1}^C \exp w_j \cdot \omega_k(x)}$, where w are classifier weights indexable by label y and C is the total number of classes.



We also apply triplet loss: $L_{Tri} = [d_{ap} - d_{an}]_+$, where d is a distance metric and a, p, n are anchor, positive and negative samples in a batch. Finally, we apply center loss [29]: $L_{Cen} = \|\omega_k(x) - c_y\|_2$, where c_y is a learnable centroid of all features belonging to class y . Using weights $0 \leq \alpha_1, \alpha_2, \alpha_3$, the overall loss is the weighted sum of these three losses over all m subheads:

$$L_{D^2FEL} = \sum_{k=1}^m [\alpha_1 L_{CE} + \alpha_2 L_{Tri} + \alpha_3 L_{Cen}] \quad (7)$$

One of the advantages of D²FEL is the simplicity in loss design. By leveraging on powerful and proven loss techniques, D²FEL avoids over-specialization and achieves all-rounded strong performance across single and cross domain Person ReID benchmarks.

4 EXPERIMENTS

Domain Generalization Person ReID Benchmarks There are a few evaluation benchmarks for DG-ReID methods. Works such as M³L [34] and DEX [1] adopt a leave-one-out evaluation, where three out of four datasets (Market-1501, DukeMTMC-reID, CUHK03 and MSMT17_V2, which we abbreviate to M, D, C and MS respectively) would be used for training and the one left out is used for testing. For example, C+D+MS implies that the method is trained on C, D and MS and tested on M. Only the training partitions of the source datasets are used for training. Four evaluations are performed, with each dataset taking turns as the target test set. Following the protocol set in M³L and DEX, for CUHK03 the classic split is used for training, while the new split is used for evaluation. Another popular way to conduct this leave-one-out evaluation is to merge the train, query and gallery partitions of the source datasets to form a larger training set, keeping the test set the same as before. We evaluate our D²FEL on the former benchmark. However, in our experiments we compare D²FEL against other methods that used the latter evaluation with more training data.

Single Domain Supervised Person ReID Benchmarks Our single domain benchmarks are more straightforward, with each of

Table 3: Results on the modern DG-ReID benchmarks. For the methods with the dagger symbol \dagger , we evaluated the official open source implementation on this benchmark. Bold numbers are the best, while underlined numbers are second.

Method	Training Data	C+D+MS → M		C+M+MS → D		C+D+M → MS		D+M+MS → C		Average	
		Rank-1	mAP								
DualNorm [12] \dagger	Train Only	78.9	52.3	68.5	51.7	37.9	15.4	28.0	27.6	53.3	36.8
QACConv [18]	Train Only	67.7	35.6	66.1	47.1	24.3	7.5	23.5	21.0	45.4	27.8
OSNet-JBN [39] \dagger	Train Only	73.4	45.1	61.5	42.3	35.7	13.7	20.9	20.9	47.9	30.5
OSNet-AIN [39] \dagger	Train Only	74.2	47.4	62.7	44.5	37.9	14.8	22.4	22.4	49.3	32.3
M ³ L [34]	Train Only	75.9	50.2	69.2	51.1	36.9	14.7	33.1	32.1	53.8	37.0
DEX [1]	Train Only	81.5	55.2	73.7	55.0	43.5	18.7	36.7	33.8	58.9	40.7
META [30] \dagger	Train Only	66.7	44.6	61.8	42.7	32.4	13.1	21.3	21.6	45.6	30.5
ACL [33] \dagger	Train Only	<u>86.1</u>	63.1	71.7	53.4	47.2	19.4	35.5	34.6	59.3	41.5
SIL [26] \dagger	Train Only	79.2	52.8	68.3	47.0	36.9	13.8	29.5	28.9	53.5	35.6
PAT [22]	Train Only	75.2	51.7	71.8	56.5	45.6	21.6	31.1	31.5	55.9	40.3
CBN [40]	Train+Test	74.7	47.3	70.0	50.1	37.0	15.4	25.2	25.7	51.7	34.6
SNR [13]	Train+Test	75.2	48.5	66.7	48.3	35.1	13.8	29.1	29.0	51.5	34.9
MECL [32]	Train+Test	80.0	56.5	70.0	53.4	32.7	13.3	32.1	31.5	53.7	38.7
RaMoE [4]	Train+Test	82.0	56.5	73.6	56.9	34.1	13.5	36.6	35.5	56.6	40.6
MixNorm [24]	Train+Test	78.9	51.4	70.8	49.9	47.2	19.4	29.6	29.0	56.6	37.4
MetaBIN [3]	Train+Test	83.2	61.2	71.3	54.9	40.8	17.0	38.1	37.5	58.4	42.7
D ² FEL-3-RP (Ours)	Train Only	85.2	61.1	<u>75.0</u>	<u>57.6</u>	<u>48.0</u>	<u>20.8</u>	37.0	<u>38.5</u>	<u>61.3</u>	<u>44.5</u>
D ² FEL-3-PCA (Ours)	Train Only	86.5	<u>62.3</u>	76.1	58.2	48.1	<u>20.8</u>	37.6	39.6	62.1	45.2

Table 4: Results on the Single Domain ReID Benchmarks. For the methods with the dagger symbol \dagger , we evaluated the official open source implementation on this benchmark. Bold numbers are the best, while underlined numbers are second.

Method	Same Domain			Domain Generalization				Omni-Domain Generalization			
	BoT \dagger	MGN \dagger	AGW	DualNorm \dagger	SIL \dagger	META \dagger	ACL \dagger	OSNet-AIN \dagger	D ² FEL-RP	D ² FEL-PCA	
Market-1501	mAP	80.6	85.3	88.2	76.4	71.9	47.2	73.1	78.5	87.2	<u>87.6</u>
	R1	92.3	94.5	95.3	91.9	88.9	75.1	88.0	92.5	<u>95.0</u>	95.0
DukeMTMC-reID	mAP	63.0	76.3	79.6	67.7	61.5	46.7	49.9	69.9	77.7	78.6
	R1	78.9	86.9	<u>89.0</u>	83.8	79.9	73.1	71.5	84.7	<u>89.0</u>	89.5
CUHK03	mAP	88.5	87.6	62.0	67.2	78.1	56.0	79.8	70.0	<u>88.6</u>	89.9
	R1	90.5	91.1	63.6	68.9	82.5	60.5	83.2	74.9	<u>91.7</u>	93.0
MSMT17 (V2)	mAP	49.2	50.5	49.3	43.9	37.2	37.1	27.7	42.7	<u>57.2</u>	61.0
	R1	74.7	74.8	68.3	74.4	66.2	69.1	57.0	71.5	<u>83.4</u>	83.8

the four Person ReID datasets used individually. In all experiments, we use mean average precision (mAP) and/or Rank-1 to quantify performance.

4.1 Implementation Details

In all experiments, we use ResNet-50 as a base model and apply cross-entropy, triplet and center losses to all subheads with $\alpha_1 = 1$, $\alpha_2 = 1$ and $\alpha_3 = 0.0005$. The learning rate starts at $1.75e-6$ and linearly warms up to $1.75e-4$ over the first 10 epochs. It is later reduced by a factor of 0.1 each in epochs 30 and 55. Applying Fully-Combinatorial-IN of depth $\delta = 3$, we deploy $2^3 = 8$ subheads of 3 bottlenecks, each expressing a unique IN-pattern (see Figure 1 for an example of D²FEL with $\delta = 2$). We use a batch size of 32, apply random erasing [38] with $p=0.1$, and color-jitter augmentation. We train for 150 epochs. For dimension reduction, we evaluate both random projections (RP) and PCA, leading to two models D²FEL-RP and D²FEL-PCA.

4.2 Results for Domain Generalization Person ReID

Table 3 compares recent DG-ReID methods with ours on the leave-one-out benchmark evaluations. D²FEL outperforms previous SOTA by 2.4% in Rank-1 and 3.2% in mAP for C+M+MS → D. For D+M+MS → C, we see a jump of 2.1% in Rank-1 and 5.0% in mAP. Our method compares favorably against recent SOTA methods that merge the train and test sets of the source domains, showing that D²FEL learns efficiently from data. It is also noteworthy that random projections perform very well with only a slight drop in performance.

4.3 Results on Single-Domain Supervised Person ReID benchmarks

Table 4 compares D²FEL against SOTA cross-domain and single-domain ReID methods on the simple single-domain supervised Person ReID benchmarks. Methods developed for DG-ReID perform

poorly when adapted back to the single domain task because they may have been over-specialized to work only on the DG-ReID setting. The simple design and strong theoretical underpinnings of D²FEL allow it to avoid this trap, achieving or even outperforming SOTA performance in all single-domain Person ReID benchmarks.

4.4 Ablation Studies

Table 5: Ablation over major components of D²FEL. Starting with a baseline, we extend it to a self-ensemble of 8 branches of depth $\delta = 3$ each and then apply Fully-Combinatorial-IN to the branches.

Config	C+D+M → MS		MSMT17	
	mAP	R1	mAP	R1
Baseline	17.4	42.2	46.7	74.6
+Self-Ens (8 Branch)	19.7	46.5	50.0	77.5
+FullComb-IN ($\delta = 3$)	20.8	48.7	61.0	83.8

4.4.1 Components of D²FEL. Starting with a baseline model, a self-ensemble (Self-Ens) framework is applied to create eight branches, each with a depth of $\delta = 3$. Next, we manifest Fully-Combinatorial-IN (FullComb-IN) by adding or removing IN for each bottleneck. Table 5 compares the performance as we add features of D²FEL to a baseline, showing that self-ensembles alone do contribute to performance, but Fully-Combinatorial-IN reaps more performance benefits through feature diversity.

Table 6: Ablation on D²FEL depth δ . For brevity, we apply random projection to $d = 2048$ and report the mAP scores.

Benchmark	D ² FEL Depth (δ)				
	0	1	2	3	4
DukeMTMC-reID	84.1	85.9	87.1	87.3	88.0
C → M	67.6	71.0	72.6	74.2	72.6
D+MS → C	20.6	22.8	23.4	25.4	25.6
C+D+M → MS	42.2	44.3	46.9	47.5	46
Average	53.6	56.0	57.5	58.6	58.1

4.4.2 Varying depths of D²FEL. Table 6 compares the effects of Fully-Combinatorial-IN for varying depths δ of D²FEL. $\delta = 0$ is the performance of a baseline model with no self-ensemble nor IN pattern diversity. As we increase depth, performance improvements are observed that eventually hit diminishing returns. Since the number of branches expressed is exponential in the depth, the computation cost of train a deeper D²FEL model grows accordingly, outweighing the diminishing benefits from more IN pattern diversity. We found $\delta = 3$ to be ideal for D²FEL.

4.4.3 Dimension Reduction Study. Figure 5 compares the performance of random projections and PCA as we reduce to smaller dimensions in D → M. Using D²FEL of depth $\delta = 3$, the 8 subheads produce a combined feature dimension of 16384. As we reduce the dimensions of these features, their performance generally holds up well for both techniques until $d < 1024$, where we see a drastic degradation of mAP for random projections. PCA, however, still continues to perform well into even lower dimensions down to $d = 256$ where the mAP has dropped by *only* 0.8% from the original performance.

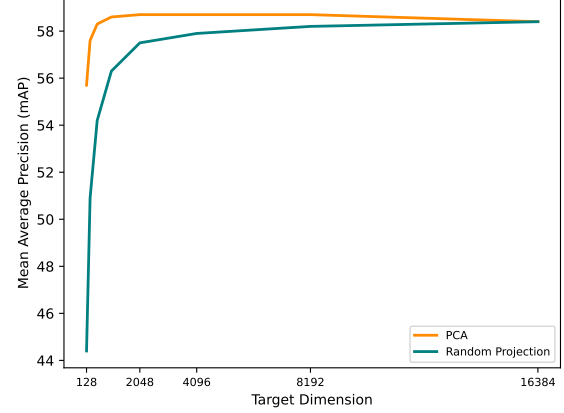


Figure 5: Comparing PCA vs. Random Projection performance on the C+D+MS → M benchmark as target dimensions are reduced. The original dimension is 16384. Down to a target dimension of around 2048, both methods are comparable.

Table 7: Comparing methods of dimension reduction. Values are mAP/Rank-1.

Benchmark	AutoEnc (L2)	AutoEnc (L1)	RandProj	PCA
Market-1501	85.7/94.7	86.0/94.9	84.6/94.5	85.5/94.8
CUHK03	89.3/92.5	89.4/93.2	86.2/90.4	87.1/89.2
D → M	37.8/67.4	38.4/68.6	40.8/72.1	42.1/72.1
M → MS	10.4/28.0	10.1/27.3	12.2/32.1	12.8/32.7

4.4.4 Deep Auto-Encoder Study. Table 7 compares the dimension reduction effectiveness between deep auto-encoders, random projections and PCA. Auto-encoder methods use a set of fully connected layers for encoding the large-dimensional feature and another set for decoding them back to the original dimension. The decoded feature is compared against the original using a reconstruction loss, which in our experiments is either a L_1 or L_2 distance loss. Auto-encoders work well only in the single-domain Person ReID tasks, but worked poorly across domains, indicating that they overfit to the source domain during training and cannot produce omni-domain generalizable encodings at test time.

5 CONCLUSION

In this work we propose the Diverse Deep Feature Ensemble Learning (D²FEL), a method that outperforms the SOTA in both single-domain supervised Person ReID and DG-ReID benchmarks. In designing D²FEL we incorporated two novel approaches. Firstly, we investigated self-ensembles in new ways to enable them for direct application in Person ReID inference. Secondly, we incorporated random projections, a technique new to Person ReID that comes from the database and text search disciplines, to efficiently and effectively reduce the large features produced by ensembles. We hope this study lays the groundwork for the development of new methods that achieve Omni-Domain Generalization in Person ReID.

ACKNOWLEDGMENTS

This work was supported by the Defence Science and Technology Agency (DSTA) Postgraduate Scholarship, of which Eugene P.W. Ang is a recipient. It was carried out at the Rapid-Rich Object Search (ROSE) Lab at the Nanyang Technological University, Singapore.

REFERENCES

- [1] Eugene Ang, Shan Lin, and Alex C. Kot. 2021. DEX: Domain Embedding Expansion for Generalized Person Re-identification. In *The 32nd British Machine Vision Conference*. 14.
- [2] Weihua Chen, Xiaotang Chen, Jianguo Zhang, and Kaiqi Huang. 2017. Beyond triplet loss: A deep quadruplet network for person re-identification. In *Proceedings - 30th IEEE Conference on Computer Vision and Pattern Recognition, CVPR 2017*, Vol. 2017-Janua. 1320–1329. <https://doi.org/10.1109/CVPR.2017.145> arXiv:1704.01719
- [3] Seocheon Choi, Taekyung Kim, Minki Jeong, Hyoungseob Park, and Changick Kim. 2021. Meta-Batch-Instance Normalization for Generalizable Person Re-Identification. In *Proceedings of the IEEE/CVF Conference on Computer Vision and Pattern Recognition (CVPR)*.
- [4] Yongxing Dai, Xiaotong Li, Jun Liu, Zekun Tong, and Ling-Yu Duan. 2021. Generalizable Person Re-identification with Relevance-aware Mixture of Experts. In *2021 Conference on Computer Vision and Pattern Recognition (CVPR)*. arXiv:2105.09156
- [5] Sanjoy Dasgupta and Anupam Gupta. 2002. An Elementary Proof of a Theorem of Johnson and Lindenstrauss. In *Random Structures and Algorithms*. 1–10. <https://doi.org/10.1002/rsa.10073>
- [6] Jia Deng, Wei Dong, Richard Socher, Li-Jia Li, Kai Li, and Li Fei-Fei. 2010. ImageNet: A large-scale hierarchical image database. In *Proc. IEEE Conference on Computer Vision and Pattern Recognition (CVPR)*. 248–255.
- [7] Karl Pearson F.R.S. 1901. LIII. On lines and planes of closest fit to systems of points in space. *The London, Edinburgh, and Dublin Philosophical Magazine and Journal of Science* 2, 11 (1901), 559–572. <https://doi.org/10.1080/14786440109462720>
- [8] Kaiming He, Xiangyu Zhang, Shaoqing Ren, and Jian Sun. 2016. Deep residual learning for image recognition. In *Proceedings of the IEEE Computer Society Conference on Computer Vision and Pattern Recognition*, Vol. 2016-Decem. 770–778. arXiv:1512.03385
- [9] Alexander Hermans, Lucas Beyer, and Bastian Leibe. 2017. In Defense of the Triplet Loss for Person Re-Identification. In *arXiv preprint*. arXiv:1703.07737 <http://arxiv.org/abs/1703.07737>
- [10] Harold Hotelling. 1933. Analysis of a complex of statistical variables into principal components. *Journal of Educational Psychology* 24 (1933), 498–520. <https://api.semanticscholar.org/CorpusID:144828484>
- [11] Yan Huang, Jingsong Xu, Qiang Wu, Zhedong Zheng, Zhaoxiang Zhang, and Jian Zhang. 2019. Multi-pseudo regularized label for generated data in person re-identification. *IEEE Transactions on Image Processing* 28, 3 (2019), 1391–1403. <https://doi.org/10.1109/TIP.2018.2874715> arXiv:1801.06742
- [12] Jieru Jia, Qiuqi Ruan, and Timothy M. Hospedales. 2020. Frustratingly easy person re-identification: Generalizing person Re-ID in practice. In *30th British Machine Vision Conference 2019, BMVC 2019*. arXiv:1905.03422
- [13] Xin Jin, Cuiling Lan, Wenjun Zeng, Zhibo Chen, and Li Zhang. 2020. Style Normalization and Restitution for Generalizable Person Re-Identification. In *Proceedings of the IEEE Computer Society Conference on Computer Vision and Pattern Recognition*. 3140–3149. arXiv:2005.11037
- [14] William Johnson and Joram Lindenstrauss. 1984. Extensions of Lipschitz maps into a Hilbert space. *Contemp. Math.* 26 (1984), 189–206. <https://doi.org/10.1090/conm/026/737400>
- [15] Xu Lan, Xiatian Zhu, and Shaogang Gong. 2018. Knowledge Distillation by On-the-Fly Native Ensemble. In *Proceedings of the 32nd International Conference on Neural Information Processing Systems (NIPS'18)*. Curran Associates Inc., Red Hook, NY, USA, 7528–7538.
- [16] Wei Li, Rui Zhao, Tong Xiao, and Xiaogang Wang. 2014. DeepReID: Deep Filter Pairing Neural Network for Person Re-identification. In *2014 IEEE Conference on Computer Vision and Pattern Recognition*. 152–159.
- [17] Zongyi Li, Yuxuan Shi, Hefei Ling, Jiazhong Chen, Qian Wang, and Fengfan Zhou. 2022. Reliability Exploration with Self-Ensemble Learning for Domain Adaptive Person Re-identification. *Proceedings of the AAAI Conference on Artificial Intelligence* 36, 2 (2022), 1527–1535. <https://doi.org/10.1609/aaai.v36i2.20043>
- [18] Shengcai Liao and Ling Shao. 2020. Interpretable and Generalizable Deep Image Matching with Adaptive Convolutions. *European Conference on Computer Vision (ECCV)* abs/1904.1 (2020). arXiv:1904.10424
- [19] Shan Lin and Chang Tsun Li. 2017. End-to-End Correspondence and Relationship Learning of Mid-Level Deep Features for Person Re-Identification. In *DICTA 2017 - 2017 International Conference on Digital Image Computing: Techniques and Applications*, Vol. 2017-Decem. 1–6. <https://doi.org/10.1109/DICTA.2017.8227426>
- [20] Shan Lin, Chang-Tsun Li, and Alex C. Kot. 2020. Multi-Domain Adversarial Feature Generalization for Person Re-Identification. *IEEE Transactions on Image Processing* (nov 2020). arXiv:2011.12563
- [21] Hao Luo, Youzhi Gu, Xingyu Liao, Shenqi Lai, and Wei Jiang. 2019. Bag of tricks and a strong baseline for deep person re-identification. In *IEEE Computer Society Conference on Computer Vision and Pattern Recognition Workshops*, Vol. 2019-June. 1487–1495. arXiv:1903.07071
- [22] Hao Ni, Yuke Li, Lianli Gao, Heng Tao Shen, and Jingkuan Song. 2023. Part-Aware Transformer for Generalizable Person Re-identification. In *Proceedings of the IEEE/CVF International Conference on Computer Vision*. 11280–11289.
- [23] Xingang Pan, Ping Luo, Jianping Shi, and Xiaou Tang. 2018. Two at Once: Enhancing Learning and Generalization Capacities via IBN-Net. In *Lecture Notes in Computer Science (including subseries Lecture Notes in Artificial Intelligence and Lecture Notes in Bioinformatics)*, Vol. 11208 LNCS. 484–500. https://doi.org/10.1007/978-3-030-01225-0_29 arXiv:1807.09441
- [24] Lei Qi, Lei Wang, Yinghuan Shi, and Xin Geng. 2022. A Novel Mix-Normalization Method for Generalizable Multi-Source Person Re-Identification. *IEEE Transactions on Multimedia* (2022), 1–12. <https://doi.org/10.1109/TMM.2022.3183393>
- [25] Jifei Song, Yongxin Yang, Yi Zhu Song, Tao Xiang, and Timothy M. Hospedales. 2019. Generalizable person re-identification by domain-invariant mapping network. In *Proceedings of the IEEE Computer Society Conference on Computer Vision and Pattern Recognition*, Vol. 2019-June. 719–728.
- [26] Wentao Tan, Changxing Ding, Pengfei Wang, Mingming Gong, and Kui Jia. 2023. Style Interleaved Learning for Generalizable Person Re-identification. *IEEE Transactions on Multimedia* (2023). <https://doi.org/10.1109/TMM.2023.3283878>
- [27] Guanshuo Wang, Yufeng Yuan, Xiong Chen, Jiwei Li, and Xi Zhou. 2018. Learning discriminative features with multiple granularities for person re-identification. In *MM 2018 - Proceedings of the 2018 ACM Multimedia Conference*. 274–282. <https://doi.org/10.1145/3240508.3240552> arXiv:1804.01438
- [28] Longhui Wei, Shiliang Zhang, Wen Gao, and Qi Tian. 2018. Person Transfer GAN to Bridge Domain Gap for Person Re-identification. In *Proceedings of the IEEE Computer Society Conference on Computer Vision and Pattern Recognition*. 79–88. <https://doi.org/10.1109/CVPR.2018.00016> arXiv:1711.08565
- [29] Yandong Wen, Kaipeng Zhang, Zhipeng Li, and Yu Qiao. 2016. A Discriminative Feature Learning Approach for Deep Face Recognition. In *Proc. European Conference on Computer Vision (ECCV)*, Vol. 9911 LNCS. Springer Science+Business Media, 499–515.
- [30] Boqiang Xian, Jian Liang, Lingxiao He, and Zhenan Sun. 2022. Mimic Embedding via Adaptive Aggregation: Learning Generalizable Person Re-identification. In *Computer Vision – ECCV 2022*, Shai Avidan, Gabriel Brostow, Moustapha Cissé, Giovanni Maria Farinella, and Tal Hassner (Eds.). Springer Nature Switzerland, Cham, 372–388.
- [31] Mang Ye, Jianbing Shen, Gaojie Lin, Tao Xiang, Ling Shao, and Steven C. H. Hoi. 2021. Deep Learning for Person Re-identification: A Survey and Outlook. *IEEE Transactions on Pattern Analysis and Machine Intelligence* (2021).
- [32] Shijie Yu, Feng Zhu, Dapeng Chen, Rui Zhao, Haobin Chen, Shixiang Tang, Jinguo Zhu, and Yu Qiao. 2021. Multiple Domain Experts Collaborative Learning: Multi-Source Domain Generalization For Person Re-Identification. arXiv:2105.12355 [cs.CV]
- [33] Pengyi Zhang, Huanzhang Dou, Yunlong Yu, and Xi Li. 2022. Adaptive Cross-domain Learning for Generalizable Person Re-identification. In *Computer Vision – ECCV 2022*, Shai Avidan, Gabriel Brostow, Moustapha Cissé, Giovanni Maria Farinella, and Tal Hassner (Eds.). Springer Nature Switzerland, Cham, 215–232.
- [34] Yuyang Zhao, Zhen Zhong, Fengxiang Yang, Zhiming Luo, Yaojin Lin, Shaozi Li, and Nicu Sebe. 2021. Learning to Generalize Unseen Domains via Memory-based Multi-Source Meta-Learning for Person Re-Identification. In *Proceedings of the IEEE Computer Society Conference on Computer Vision and Pattern Recognition*. 6273–6282. <https://doi.org/10.1109/CVPR46437.2021.00621> arXiv:2012.00417
- [35] Liang Zheng, Liyue Shen, Lu Tian, Shengjin Wang, Jingdong Wang, and Qi Tian. 2015. Scalable person re-identification: A benchmark. In *Proceedings of the IEEE International Conference on Computer Vision*, Vol. 2015 Inter. 1116–1124.
- [36] Liang Zheng, Yi Yang, and Alexander G. Hauptmann. 2016. Person Re-identification: Past, Present and Future. *arXiv preprint* (2016). arXiv:1610.02984 <http://arxiv.org/abs/1610.02984>
- [37] Zhenzhong Zheng, Liang Zheng, and Yi Yang. 2017. Unlabeled Samples Generated by GAN Improve the Person Re-identification Baseline in Vitro. In *Proceedings of the IEEE International Conference on Computer Vision*, Vol. 2017-Octob. 3774–3782. arXiv:1701.07717
- [38] Zhenzhong Zheng, Liang Zheng, Guoliang Kang, Shaozi Li, and Yi Yang. 2020. Random erasing data augmentation. In *AAAI 2020 - 34th AAAI Conference on Artificial Intelligence*. 13001–13008. <https://doi.org/10.1609/aaai.v34i07.7000> arXiv:1708.04896
- [39] Kaiyang Zhou, Yongxin Yang, Andrea Cavallaro, and Tao Xiang. 2021. Learning Generalisable Omni-Scale Representations for Person Re-Identification. In *IEEE Transactions on Pattern Analysis and Machine Intelligence*. <https://doi.org/10.1109/TPAMI.2021.3069237> arXiv:1910.06827
- [40] Zijie Zhuang, Longhui Wei, Lingxi Xie, Tianyu Zhang, Hengheng Zhang, Haozhe Wu, Haizhou Ai, and Qi Tian. 2020. Rethinking the Distribution Gap of Person Re-identification with Camera-Based Batch Normalization. In *European Conference on Computer Vision*. Springer, 140–157.